Available online at www.sciencedirect.com
SCIENCE DIRECT®
Physica D 203 (2005) 209–223
PHYSICA D
www.elsevier.com/locate/physd

Reconstruction of time-delayed feedback systems from time series

M.D. Prokhorov [a,*], V.I. Ponomarenko [a,b], A.S. Karavaev [b], B.P. Bezruchko [a,b]

[a] *Saratov Department of the Institute of RadioEngineering and Electronics, Russian Academy of Sciences, Zelyonaya Street 38, Saratov 410019, Russia*
[b] *Department of Nonlinear Processes, Saratov State University, Astrakhanskaya Street 83, Saratov 410012, Russia*

Received 27 April 2004; received in revised form 13 February 2005; accepted 28 March 2005
Available online 13 April 2005
Communicated by M. Ding

Abstract

For various classes of time-delay systems we propose the methods of their model delay-differential equation reconstruction from time series. The methods are based on the characteristic location of extrema in the time series of time-delay systems and the projection of infinite-dimensional phase space of these systems to suitably chosen low-dimensional subspaces. We verify our methods by using them for the recovery of time-delay differential equations from their chaotic solutions and for modelling experimental systems with delay-induced dynamics from their chaotic time series.

PACS: 05.45.−a; 05.45.Tp

Keywords: Parameter estimation; Delay-differential equations; Time series analysis; Nonlinear delayed feedback system

1. Introduction

Systems, whose dynamics is affected not only by the current state, but also by past states, are wide spread in nature [1]. Usually these systems are modelled by delay-differential equations. Such models are successfully used in many scientific disciplines, like physics, physiology, biology, economics and cognitive sciences. Typical examples include population dynamics [2], where individuals participate in the reproduction of a species only after maturation, or spatially extended systems, where signals have to cover distances with finite velocities [3]. Within this rather broad class of systems, one can find the Ikeda equation [4] modelling the passive optical resonator system, the Lang–Kobayashi equations [5] describing semiconductor lasers with optical feedback, the Mackey–Glass equation [6] modelling the production of red blood cells, and many other

* Corresponding author. Tel.: +7 8452 511 180; fax: +7 8452 261 156.
E-mail address: sbire@sgu.ru (M.D. Prokhorov).

0167-2789/$ – see front matter © 2005 Elsevier B.V. All rights reserved.
doi:10.1016/j.physd.2005.03.013

models in biosciences for different phenomena from glucose metabolism to infectious diseases [7].

Generally, the time-delay systems are described by the following equation

$$\varepsilon_n x^{(n)}(t) + \varepsilon_{n-1} x^{(n-1)}(t) + \cdots + \varepsilon_1 \dot{x}(t) = F(x(t), x(t-\tau_1), \ldots, x(t-\tau_k)), \quad (1)$$

where $x(t)$ is the system state at time t, $x^{(n)}(t)$ is the time derivative of order n, $\tau_1, \ldots, \tau_k$ are the delay times and $\varepsilon_1, \ldots, \varepsilon_n$ are the parameters characterizing the inertial properties of the system. To uniquely define the system (1) behaviour it is necessary to prescribe the initial conditions in the entire time interval $[-\tau_k, 0]$. Therefore, the phase space of the system has to be considered as infinite-dimensional. In fact, even first-order delay-differential equations can possess high-dimensional chaotic dynamics [8]. Thus, the direct reconstruction of the system by the time-delay embedding techniques runs into severe problems. For a successful recovery of the time-delay systems one has to use special methods. The most of them are based on the projection of the infinite-dimensional phase space of time-delay systems onto low-dimensional subspaces. These methods use different criteria of quality for the reconstructed equations, for example, the minimal forecast error of constructed model [9–12], the minimal value of information entropy [13] or various measures of complexity of the projected time series [14–18]. Several methods of time-delay system recovery exploit regression analysis [19–21].

In this paper we present the original procedure of the delay time reconstruction based on a statistical analysis of time intervals between extrema in the time series and develop further the methods of time-delay system parameter estimation from time series proposed by us recently [22,23] for a more wide class of time-delay systems including time-delay systems of high order and with several coexisting delays. We propose also the methods for reconstructing ring-type time-delay systems from time series of various dynamical variables obtained from different points of the time-delay system.

2. Peculiarities of time-delay system time series

Statistical analysis of time intervals between extrema in time series of various model and real time-delay systems reveals the following general regularities. If the system has inertial properties, the dependence of number N of pairs of extrema in its time series separated in time by τ on the value of τ demonstrates a pronounced minimum at the level of the delay time of the system (Fig. 1(a)). Let us explain the qualitative features of $N(\tau)$ with one of the most popular delay-differential equation

$$\varepsilon_1 \dot{x}(t) = -x(t) + f(x(t-\tau_1)). \quad (2)$$

In general case Eq. (2) is a mathematical model of an oscillating system composed of a ring with three ideal elements: nonlinear, delay, and inertial ones (Fig. 2). In the presence of inertial properties ($\varepsilon_1 > 0$), which corresponds to real situations, the extrema in $x(t)$ are close to quadratic ones and therefore $\dot{x}(t) = 0$ and

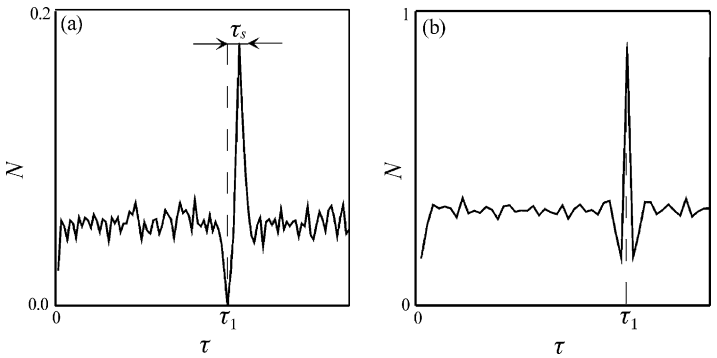

Fig. 1. Typical dependence of number N of pairs of extrema in chaotic time series of a time-delay system separated in time by τ on the value of τ in the presence of inertial properties in the system (a) and in the absence of inertial properties (b). $N(\tau)$ is normalized to the total number of extrema in time series.

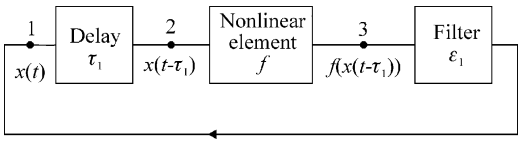

Fig. 2. Block scheme of a ring system with nonlinear time-delayed feedback. Arabic numerals designate points where a dynamical variable can be measured.

$\ddot{x}(t) \neq 0$ at the extremal points. In fact, the condition $\dot{x}(t) = \ddot{x}(t) = 0$ is satisfied for a point, which is a point of inflection, or a non-quadratic extremum, or belongs to an interval of constant value of the dynamical variable. But the presence of inertial properties in the system prevents the implementation of these conditions. It can be shown that in this case there are practically no extrema in $x(t)$ separated in time by the delay time τ_1. Differentiation of Eq. (2) with respect to t gives

$$\varepsilon_1 \ddot{x}(t) = -\dot{x}(t) + \frac{\mathrm{d}f(x(t-\tau_1))}{\mathrm{d}x(t-\tau_1)}\dot{x}(t-\tau_1). \tag{3}$$

If for $\dot{x}(t) = 0$ in a typical case $\ddot{x}(t) \neq 0$, then, as it can be seen from Eq. (3), for $\varepsilon_1 \neq 0$ the condition $\dot{x}(t-\tau_1) \neq 0$ must be fulfilled. Thus, there must be no extremum separated in time by τ_1 from a quadratic extremum and, hence, $N(\tau_1) \to 0$.

Similar properties are inherent in a more general class of time-delay systems

$$\dot{x}(t) = F(x(t), x(t-\tau_1)). \tag{4}$$

Time differentiation of Eq. (4) gives

$$\ddot{x}(t) = \frac{\partial F(x(t), x(t-\tau_1))}{\partial x(t)}\dot{x}(t) + \frac{\partial F(x(t), x(t-\tau_1))}{\partial x(t-\tau_1)} \times \dot{x}(t-\tau_1). \tag{5}$$

Similarly to Eq. (3), Eq. (5) implies that in a typical case of quadratic extrema derivatives $\dot{x}(t)$ and $\dot{x}(t-\tau_1)$ do not vanish simultaneously, i.e., if $\dot{x}(t) = 0$, then $\dot{x}(t-\tau_1) \neq 0$.

In the absence of inertial properties ($\varepsilon_1 = 0$) differentiation of Eq. (2) with respect to t gives

$$\dot{x}(t) = \frac{\mathrm{d}f(x(t-\tau_1))}{\mathrm{d}x(t-\tau_1)}\dot{x}(t-\tau_1). \tag{6}$$

From Eq. (6) it follows that if $\dot{x}(t-\tau_1) = 0$, then $\dot{x}(t) = 0$. Thus, for $\varepsilon_1 = 0$ every extremum of $x(t)$ is followed within the time τ_1 by the extremum. As the result, $N(\tau)$ shows a maximum for $\tau = \tau_1$ (Fig. 1(b)). If the system has a bounded bandpass ($\varepsilon_1 > 0$), the most probable value of the time interval between extrema in $x(t)$ shifts from τ_1 to larger values and the extrema can be found most often at the distance $\tau_1 + \tau_s$ apart (Fig. 1(a)).

The presence of noise in time series brings into existence spurious extrema that are not caused by the intrinsic dynamics of a time-delay system. Thus, owing to high-frequency noise a probability to find a pair of extrema in time series separated in time by τ has to increase in general. As a result, with noise increasing the average N value becomes greater. The probability to find a pair of extrema separated by the interval τ_1 also increases. However, for moderate noise levels this probability is still less than the probability to find a pair of extrema separated in time by $\tau \neq \tau_1$. Hence, the qualitative features of the $N(\tau)$ plot specified by the delay-induced dynamics are retained for a moderate noise level.

3. Reconstruction of first-order time-delay systems

Let us consider the procedure of first-order time-delay system recovery with Eq. (2) as an example. To define the delay time τ_1 one has to determine the extrema in the time series and after that to define for different values of time τ the number N of pairs of extrema separated in time by τ and to construct the $N(\tau)$ plot. The absolute minimum of $N(\tau)$ located near the absolute maximum is observed at the delay time τ_1. The dependence of accuracy of the delay time recovery on the step of τ variation and the time series length is considered in Ref. [22].

To recover the parameter ε_1 and the nonlinear function f from the chaotic time series let us rewrite Eq. (2) as

$$\varepsilon_1 \dot{x}(t) + x(t) = f(x(t-\tau_1)). \tag{7}$$

Thus, it is possible to reconstruct the nonlinear function by plotting in a plane a set of points with coordinates $(x(t-\tau_1), \varepsilon_1\dot{x}(t) + x(t))$. Since the parameter ε_1 is a priori unknown, one needs to plot $\varepsilon\dot{x}(t) + x(t)$ versus $x(t-\tau_1)$ under variation of ε, searching for a single-valued dependence in the $(x(t-\tau_1), \varepsilon\dot{x}(t) + x(t))$ plane, which is possible only for $\varepsilon = \varepsilon_1$. As a quan-

titative criterion of single-valuedness in searching for ε_1 we use the minimal length of a line $L(\varepsilon)$ connecting all points ordered with respect to $x(t-\tau_1)$ in the plane $(x(t-\tau_1), \varepsilon\dot{x}(t)+x(t))$. The minimum of $L(\varepsilon)$ is observed at $\varepsilon=\varepsilon_1$. The set of points constructed for the defined ε_1 in the plane $(x(t-\tau_1), \varepsilon_1\dot{x}(t)+x(t))$ reproduces the nonlinear function, which can be approximated if necessary. In contrast to methods presented in Refs. [15,16], which use only extremal points or points selected according to a certain rule for the nonlinear function recovery, the proposed technique uses all points of the time series. It allows one to estimate the parameter ε_1 and to reconstruct the nonlinear function from short time series even in the regimes of weakly developed chaos.

To test the efficiency of the proposed technique we have used it to reconstruct the equations of various time-delay systems having the form of Eq. (2) from the time series gained from their numerical solution. In particular, we apply the method to a time series of the Ikeda equation [4]

$$\dot{x}(t) = -x(t) + \mu \sin(x(t-\tau_1) - x_0) \tag{8}$$

modelling the passive optical resonator system. The Ikeda Eq. (8) has the form of Eq. (2) with $\varepsilon_1 = 1$. The parameters of the system (8) are chosen to be $\mu = 20$, $\tau_1 = 2$, $x_0 = \pi/3$ to produce a dynamics on a high-dimensional chaotic attractor [3]. Part of the time series is shown in Fig. 3(a). The time series is sampled in such a way that 200 points in time series cover a period of time equal to the delay time $\tau_1 = 2$. The data set consists of 20,000 points and exhibits about 1100 extrema.

For various τ values we count the number N of situations when $\dot{x}(t)$ and $\dot{x}(t-\tau)$ are simultaneously equal to zero and construct the $N(\tau)$ plot (Fig. 3(b)). The step of τ variation in Fig. 3(b) is equal to the integration step $h = 0.01$. The time derivatives $\dot{x}(t)$ are estimated from the time series by applying a local parabolic approximation. The absolute minimum of $N(\tau)$ takes place exactly at $\tau = \tau_1 = 2.00$. To construct the $L(\varepsilon)$ plot (Fig. 3(c)) the step of ε variation is also set by 0.01. The minimum of $L(\varepsilon)$ takes place accurately at $\varepsilon = \varepsilon_1 = 1.00$. In Fig. 3(d) the recovered nonlinear function is shown. It coincides practically with the true function of Eq. (8). Note, that for the construction of the $L(\varepsilon)$ plot and for the recovery of the multimodal function f we use only 2000 points of the time series. For the approximation of the recovered function we use polynomials of different degree. The sinusoid amplitude (Fig. 3(d)) allows one to define the parameter μ of Eq. (8). The parameter x_0 can be calculated from the function value at $x(t-\tau_1) = 0$. The approximation of the recovered function with a polynomial of degree 20 allows us to obtain

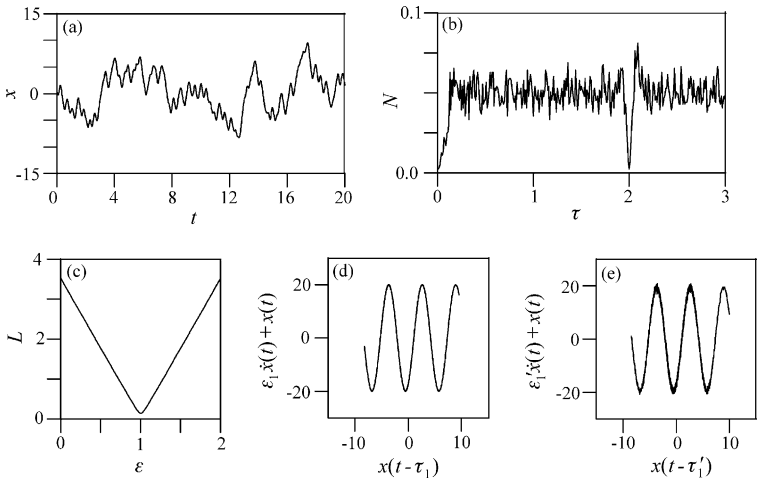

Fig. 3. (a) The time series of the Ikeda Eq. (8). (b) Number N of pairs of extrema in the time series separated in time by τ, as a function of τ. $N(\tau)$ is normalized to the total number of extrema in the time series. $N_{\min}(\tau) = N(2.00)$. (c) Length L of a line connecting all points ordered with respect to $x(t-\tau_1)$ in the $(x(t-\tau_1), \varepsilon\dot{x}(t)+x(t))$ plane, as a function of ε. $L(\varepsilon)$ is normalized to the number of points in the plane. $L_{\min}(\varepsilon) = L(1.00)$. (d) The recovered nonlinear function. (e) The nonlinear function recovered from the data corrupted by additive Gaussian white noise for noise level of 20%.

the following estimation: $\mu' = 19.94$ and $x'_0 = 1.046$ ($\pi/3 \approx 1.047$).

To investigate the robustness of the method to perturbations we apply it to the data produced by adding a zero-mean Gaussian white noise to the time series of Eq. (8). For the case where the additive noise has a standard deviation of 20% of the standard deviation of the data without noise (the signal-to-noise ratio is about 14 dB) the location of the minimum of $N(\tau)$ still allows us to estimate the delay time accurately, $\tau'_1 = 2.00$. The minimum of $L(\varepsilon)$ takes place at $\varepsilon'_1 = 0.98$. The nonlinear function recovered using the estimated values τ'_1 and ε'_1 is shown in Fig. 3(e). In spite of sufficiently high noise level and inaccuracy of estimation of ε_1 the recovery of the nonlinear function has a good quality, which is significantly higher than that reported in Ref. [21] for the same parameter values of the Ikeda equation with noise.

The second example is the method application to experimental time series of the electronic oscillator with delayed feedback. In the block representation of this oscillator (Fig. 2) a delay for time τ_1 is provided by a delay line, the role of nonlinear element is played by an amplifier with the transfer function f and the system inertial properties are defined by a filter, which parameters specify ε_1. For the case when the filter is a low-frequency first-order RC-filter such oscillator is given by

$$RC\dot{V}(t) = -V(t) + f(V(t - \tau_1)), \tag{9}$$

where $V(t)$ and $V(t - \tau_1)$ are the delay line input and output voltages, respectively; R and C are the resistance and capacitance of the filter elements. Eq. (9) is of form (2) with $\varepsilon_1 = RC$.

At $\tau_1 = 31.7$ ms and $\varepsilon_1 = 1.007$ ms we record the signal $V(t)$ (Fig. 4(a)) using an analog-to-digital converter with the sampling frequency $f_s = 4$ kHz. Since the delay time τ_1 is not a multiple of the sampling time $T_s = 0.25$ ms, the recovery of τ_1 cannot be absolutely accurate. For the step of τ variation equal to T_s, the absolute minimum of $N(\tau)$ takes place at $\tau'_1 = 31.75$ ms (Fig. 4(b)). The $L(\varepsilon)$ plot, constructed with τ'_1 and the step of ε variation equal to 0.025 ms, demonstrates the minimum at $\varepsilon'_1 = 1.000$ ms (Fig. 4(c)). The recovered nonlinear function (Fig. 4(d)) coincides practically with the true transfer function of the amplifier.

Besides the $L(\varepsilon)$ plot we use two another criteria of quality for the system recovery. The first of them exploits synchronization of unidirectionally coupled time-delay systems. We try to synchronize the recovered model equation with the experimental system (9)

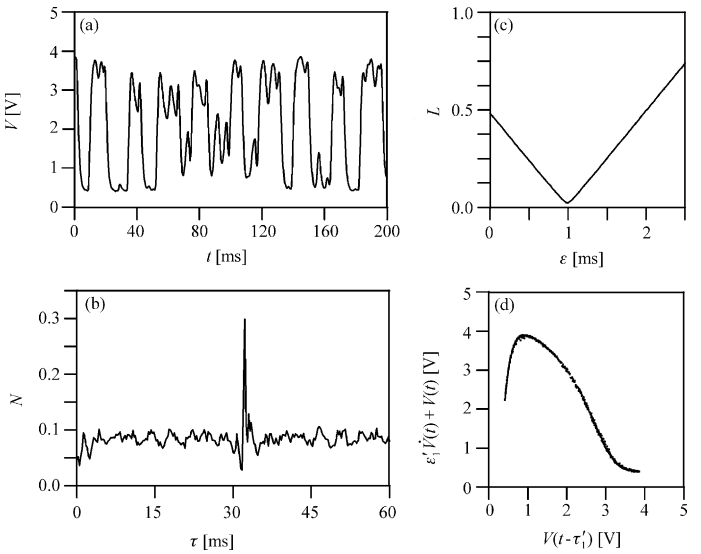

Fig. 4. (a) Experimental time series of the electronic oscillator with delayed feedback. (b) Number N of pairs of extrema in the time series separated in time by τ, as a function of τ. $N(\tau)$ is normalized to the total number of extrema in the time series. $N_{\min}(\tau) = N(31.75\,\text{ms})$. (c) The $L(\varepsilon)$ plot. $L(\varepsilon)$ is normalized to the number of points. $L_{\min}(\varepsilon) = L(1.000\,\text{ms})$. (d) The recovered nonlinear function.

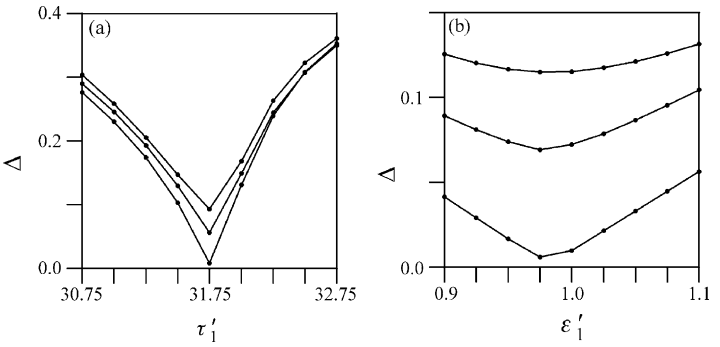

Fig. 5. (a) Synchronization error Δ as a function of τ_1'. (b) Synchronization error Δ as a function of ε_1'. From bottom to top, the curves refer to the additive noise level of 0%, 1% and 10%, respectively.

applying the following synchronization scheme [24]:

$$\varepsilon_1'\dot{y}(t) = -y(t) + f'(y(t-\tau_1')) + k(V(t) - y(t)), \tag{10}$$

where $y(t)$ is the model variable, τ_1' and ε_1' are the recovered parameters, f' is the polynomial approximation of the reconstructed nonlinear function and k is the coupling coefficient. If the recovered model parameters are close to the true ones and the coupling coefficient k is sufficiently large, the response system (10) rapidly synchronizes with the driving system (9). To quantify the measure of synchronization we calculate the synchronization error $\Delta = \langle |V(t) - y(t)| \rangle$, where $\langle \cdot \rangle$ denotes a time average.

Fig. 5(a) shows the dependence of Δ on the model parameter τ_1' varied in the vicinity of $\tau_1' = 31.75$ ms with the step of variation equal to T_s. To construct this plot we use $k = 0.5$, $\varepsilon_1' = 1.000$ ms and approximation of the recovered function f' with a polynomial of degree 11. The value of Δ is computed after transients and is averaged over 2.5 s. The minimum of Δ is observed at $\tau_1' = 31.75$ ms as well as the minimum of $N(\tau)$. We also calculate the dependence of Δ on τ_1' after adding Gaussian white noise to the time series of the driving system. For the noise level of 1% and 10% the minimum of $\Delta(\tau_1')$ still takes place at $\tau_1' = 31.75$ ms (Fig. 5(a)). Note that for the construction of $\Delta(\tau_1')$ in the presence of noise we use ε_1' and f' recovered from noisy time series.

In a similar way we plot the dependence of Δ on the model parameter ε_1' varied in the vicinity of $\varepsilon_1' = 1.000$ ms with the step of variation equal to 0.025 ms (Fig. 5(b)). The minimum of $\Delta(\varepsilon_1')$ is observed at $\varepsilon_1' = 0.975$ ms which is slightly below the estimation of ε_1' obtained from the $L(\varepsilon)$ plot. This distinction between ε_1' estimations can result from inaccuracy of f' approximation performed for calculation of Δ. For the driving signal corrupted by additive Gaussian white noise of 1% and 10% the minimum of $\Delta(\varepsilon_1')$ is again observed at $\varepsilon_1' = 0.975$ ms (Fig. 5(b)). As can be seen from Fig. 5, the inaccuracy of the delay time estimation gives a greater synchronization error than the inaccuracy of estimation of ε_1.

The next quantitative measure of accuracy used in our paper for the recovered model is the one-step forecast error $\sigma = \langle |V(t) - y(t)| \rangle$, where $V(t)$ is the experimentally measured variable, $y(t)$ is the variable of the model having the form of Eq. (10) with $k = 0$, and $\langle \cdot \rangle$ denotes a time average. This measure shows how the model with the recovered τ_1', ε_1', and f' fits the observed data if the initial conditions for the one-step prediction are chosen from the experimental time series. The dependencies of σ on the parameters τ_1' and ε_1' are qualitatively similar to the dependencies $\Delta(\tau_1')$ and $\Delta(\varepsilon_1')$ (Fig. 5), respectively, and are not shown here.

4. Peculiarities of ring time-delay system reconstruction

In the ring time-delay systems described by Eq. (2) a dynamical variable can be measured at different points indicated in Fig. 2 by the numerals 1–3. However, it should be mentioned that in the real systems it is not

always possible to localize the elements depicted in Fig. 2 or to choose the point of measurement because of the integrity of the system. The delayed feedback system recovery for the case when the observed dynamical variable is $x(t)$ measured at the point 1 has been considered in Section 3.

In the case, when the observed dynamical variable is $x(t-\tau_1)$ measured at the point 2 (Fig. 2), one can use the same procedure for estimation of the system parameters as in the case of $x(t)$ measurement since the observable is simply shifted in time by the delay time τ_1 about $x(t)$. For example, reconstructing the electronic oscillator with delayed feedback described by Eq. (9) from experimental time series of voltage $V(t-\tau_1)$ at the delay line output we obtain the results qualitatively similar to those presented in Fig. 4 for the case of the system recovery from the time series of $V(t)$.

Let us consider a technique of the time-delay system (2) reconstruction for the third possible case, when the observed variable is $f(x(t-\tau_1))$ measured at the point 3 (Fig. 2). As well as in the time series of $x(t)$, there are practically no extrema separated in time by τ_1 in the time series of the variable $f(x(t-\tau_1))$, since $\mathrm{d}f(x(t-\tau_1))/\mathrm{d}t = (\mathrm{d}f(x(t-\tau_1))/\mathrm{d}x)\dot{x}(t-\tau_1)$. Then, the delay time τ_1 can be estimated by the location of the absolute minimum in the $N(\tau)$ plot constructed from the variable $f(x(t-\tau_1))$.

The nonlinear function f can be recovered by plotting $f(x(t-\tau_1))$ versus $x(t-\tau_1)$. To obtain the unknown values of $x(t-\tau_1)$ one has to filter the chaotic time series of the variable $f(x(t-\tau_1))$ with a low-frequency first-order filter with the cut-off frequency $\nu_1 = 1/\varepsilon_1$ and to shift the signal $x(t)$ at the filter output by the delay time τ_1 defined earlier. Since the parameter ε_1 and correspondingly the value of ν_1 are a priori unknown, we filter the time series of $f(x(t-\tau_1))$ under variation of the filter cut-off frequency $\nu = 1/\varepsilon$ and plot $f(x(t-\tau_1))$ versus $u(t-\tau_1)$, where $u(t-\tau_1)$ is the signal at the filter output shifted by the time τ_1. Note, that a single-valued dependence in the plane $(u(t-\tau_1), f(x(t-\tau_1)))$ is possible only for $\varepsilon = \varepsilon_1$. In this case $u(t-\tau_1) = x(t-\tau_1)$ and the set of points constructed in the plane reproduces the function f, which can be approximated if necessary. As a quantitative criterion of single-valuedness in searching for ε_1 we use again the minimal length of a line $L(\varepsilon)$ connecting all points in the plane $(u(t-\tau_1), f(x(t-\tau_1)))$ ordered with respect to $u(t-\tau_1)$. The minimum of $L(\varepsilon)$ is observed at $\varepsilon = \varepsilon_1$.

We apply the method to time series of the variable $f(x(t-\tau_1))$ of the Mackey–Glass equation [6]

$$\dot{x}(t) = -bx(t) + \frac{ax(t-\tau_1)}{1+x^c(t-\tau_1)}, \tag{11}$$

which can be converted to Eq. (2) by division by b. The parameters of the system (11) are chosen to be $a = 0.2$, $b = 0.1$, $c = 10$ and $\tau_1 = 300$ to produce a dynamics on a high-dimensional chaotic attractor [8]. Part of the time series is shown in Fig. 6(a). The location of the absolute minimum of $N(\tau)$ (Fig. 6(b)) allows us to recover the delay time, $\tau_1' = 300$. The step of τ variation in Fig. 6(b) is equal to the integration step $h = 1$. The minimum of $L(\varepsilon)$ (Fig. 6(c)) takes place at $\varepsilon_1' = 10.0$ ($\varepsilon_1 = 1/b = 10$). To construct the $L(\varepsilon)$ plot we use the step of ε variation equal to 0.1. The nonlinear function recovered using the estimated τ_1' and ε_1' (Fig. 6(d)) coincides practically with the true nonlinear function.

5. Reconstruction of time-delay systems of high order

The method of the delay time definition based on the statistical analysis of time intervals between extrema in the time series can be extended to time-delay systems of high order

$$\varepsilon_n x^{(n)}(t) + \varepsilon_{n-1}x^{(n-1)}(t) + \cdots + \varepsilon_1\dot{x}(t) = F(x(t), x(t-\tau_1)). \tag{12}$$

Time differentiation of Eq. (12) gives

$$\varepsilon_n x^{(n+1)}(t) + \varepsilon_{n-1}x^{(n)}(t) + \cdots + \varepsilon_1\ddot{x}(t) = \frac{\partial F(x(t), x(t-\tau_1))}{\partial x(t)}\dot{x}(t) + \frac{\partial F(x(t), x(t-\tau_1))}{\partial x(t-\tau_1)} \times \dot{x}(t-\tau_1). \tag{13}$$

For $\dot{x}(t) = 0$ the condition $\dot{x}(t-\tau_1) \neq 0$ will be satisfied if the left-hand side of Eq. (13) does not vanish. If a probability to obtain zero in the left-hand side of Eq. (13) is very small for the extremal points, the $N(\tau)$ plot qualitatively must have a shape similar to that inherent in the case of first-order delay-differential equations such as Eqs. (2) and (4).

We have found out that for sufficiently small values of ε_i, $i = 1, \ldots, n$, the $N(\tau)$ plot demonstrates the absolute minimum at $\tau = \tau_1$ as well in the case of the

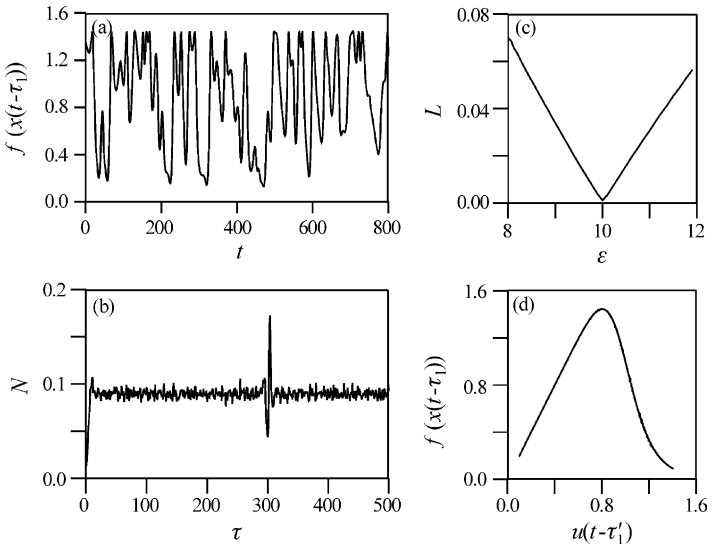

Fig. 6. (a) The time series of the variable $f(x(t-\tau_1))$ of the Mackey–Glass system. (b) Number N of pairs of extrema in the time series of $f(x(t-\tau_1))$ separated in time by τ, as a function of τ. $N(\tau)$ is normalized to the total number of extrema in the time series. $N_{\min}(\tau) = N(300)$. (c) Length L of a line connecting points ordered with respect to $u(t-\tau_1')$ in the plane $(u(t-\tau_1'),\ f(x(t-\tau_1)))$, as a function of ε. $L(\varepsilon)$ is normalized to the number of points. $L_{\min}(\varepsilon) = L(10.0)$. (d) The recovered nonlinear function.

first-order time-delay systems. The distribution of the values of the left-hand side of Eq. (13) at the extremal points has a pronounced minimum in the neighbourhood of zero in this case. As the parameters ε_i increase, the absolute minimum of $N(\tau)$ shifts from τ_1 to larger values. The greater are ε_i characterizing the influence of the system inertial elements, the greater is the shift. This time shift of $N(\tau)$ minimum does not depend on τ_1. Note that in the first-order time-delay systems the location of the absolute minimum in the $N(\tau)$ plot does not depend on ε_1.

The proposed method of the parameter ε_1 estimation and the nonlinear function recovery based on the projection of infinite-dimensional phase space of the time-delay system to suitably chosen two-dimensional subspaces can be also applied to a variety of time-delay systems of order higher than that of Eq. (2). For instance, if the dynamics of a time-delay system is governed by the second-order delay-differential equation

$$\varepsilon_2\ddot{x}(t) + \varepsilon_1\dot{x}(t) = -x(t) + f(x(t-\tau_1)), \tag{14}$$

the nonlinear function can be reconstructed by plotting in a plane a set of points with coordinates $(x(t-\tau_1), \varepsilon_2\ddot{x}(t) + \varepsilon_1\dot{x}(t) + x(t))$. Since the parameters ε_1 and ε_2 are a priori unknown, one needs to plot $\hat{\varepsilon}_2\ddot{x}(t) + \hat{\varepsilon}_1\dot{x}(t) + x(t)$ versus $x(t-\tau_1)$ under variation of $\hat{\varepsilon}_1$ and $\hat{\varepsilon}_2$, searching for a single-valued dependence, which is possible only for $\hat{\varepsilon}_1 = \varepsilon_1$, $\hat{\varepsilon}_2 = \varepsilon_2$. In this search for ε_1 and ε_2 we calculate the length of a line $L(\hat{\varepsilon}_1, \hat{\varepsilon}_2)$ connecting points ordered with respect to $x(t-\tau_1)$ in the plane $(x(t-\tau_1), \hat{\varepsilon}_2\ddot{x}(t) + \hat{\varepsilon}_1\dot{x}(t) + x(t))$. The minimum of $L(\hat{\varepsilon}_1, \hat{\varepsilon}_2)$ is observed at $\hat{\varepsilon}_1 = \varepsilon_1$, $\hat{\varepsilon}_2 = \varepsilon_2$. The set of points constructed in the plane for these defined values of ε_1 and ε_2 reproduces the nonlinear function.

The methods of reconstruction of second-order time-delay systems from scalar time series have been considered in Refs. [10,17,18]. However, these methods deal only with the recovery of the delay time and the nonlinear function. For the recovery of the latter one they use only the points of the phase space section. As the result, these methods need long time series for qualitative reconstruction of the nonlinear function. The proposed by us procedure of the delay time estimation based on the statistical analysis of time intervals between extrema in the time series needs significantly smaller time of computation than the methods of the delay time definition based on calculation of the fill-

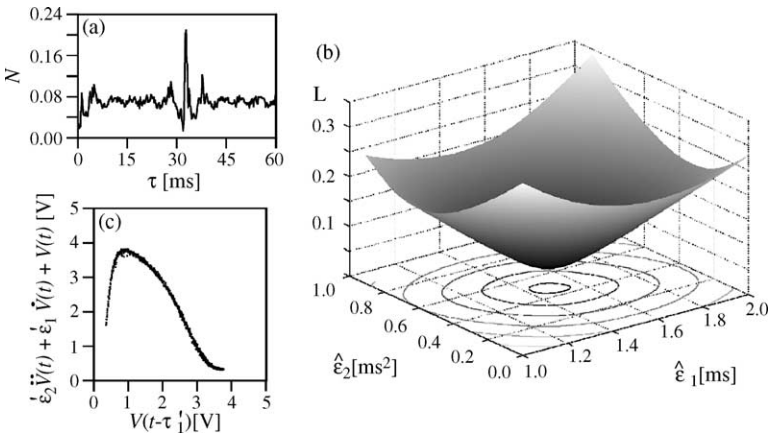

Fig. 7. Reconstruction of the electronic oscillator with delayed feedback with a two-section filter. (a) Number N of pairs of extrema in the experimental time series separated in time by τ normalized to the total number of extrema. $N_{\min}(\tau) = N(31.75\,\text{ms})$. (b) The $L(\hat{\varepsilon}_1, \hat{\varepsilon}_2)$ plot normalized to the number of points. $L_{\min}(\hat{\varepsilon}_1, \hat{\varepsilon}_2) = L(1.48\,\text{ms}, 0.48\,\text{ms}^2)$. (c) The recovered nonlinear function.

ing factor of the projected time series [17] and minimization of the one-step forecast error of the recovered model equation [10,18].

To verify the method efficiency we have applied it to experimental time series gained from the electronic oscillator with delayed feedback that is similar to that considered in Section 3, but contains two identical low-frequency in-series RC-filters. The dynamics of this oscillator is governed by Eq. (14), where $x(t)$ and $x(t-\tau_1)$ are the delay line input and output voltages, respectively, $\varepsilon_1 = R_1C_1 + R_2C_2$, $\varepsilon_2 = R_1C_1R_2C_2$, and R_1, R_2, C_1 and C_2 are respectively the resistances and capacitances of the first and the second filters.

Using the analog-to-digital converter we record with the sampling frequency 4 kHz the time series of voltage at the delay line input for $\tau_1 = 31.7\,\text{ms}$, $R_1C_1 = 1.007\,\text{ms}$ and $R_2C_2 = 0.479\,\text{ms}$ ($\varepsilon_1 = 1.486\,\text{ms}$ and $\varepsilon_2 = 0.482\,\text{ms}^2$). The absolute minimum of $N(\tau)$ is observed at $\tau_1' = 31.75\,\text{ms}$ (Fig. 7(a)). The $L(\hat{\varepsilon}_1, \hat{\varepsilon}_2)$ plot, constructed with the step of $\hat{\varepsilon}_1$ variation equal to 0.01 ms and the step of $\hat{\varepsilon}_2$ variation equal to $0.01\,\text{ms}^2$, demonstrates the minimum at $\varepsilon_1' = 1.48\,\text{ms}$ and $\varepsilon_2' = 0.48\,\text{ms}^2$ (Fig. 7(b)). These ε_1' and ε_2' values give the following estimation of the filter parameters: $(R_1C_1)' = 1.00\,\text{ms}$ and $(R_2C_2)' = 0.48\,\text{ms}$. The recovered nonlinear function (Fig. 7(c)) coincides with a good accuracy with the true transfer function of the nonlinear element.

With the recovered parameters ε_1' and ε_2' we plot the distribution of the sum $\varepsilon_2'\dddot{x}(t) + \varepsilon_1'\ddot{x}(t)$ using all points of the time series (Fig. 8(a)). The maximum of this distribution is observed close to zero. The distribution of the same sum constructed using only the extremal points $\dot{x}(t) = 0$ demonstrates a pronounced minimum in the vicinity of zero (Fig. 8(b)). This result counts in favour of the conclusion that the probability to obtain zero in the left-hand side of Eq. (13) is sufficiently small at the extremal points. The presence of minimum in the vicinity of zero in Fig. 8(b) agrees well with the existence of minimum at the delay time of the system in the $N(\tau)$ plot (Fig. 7(a)).

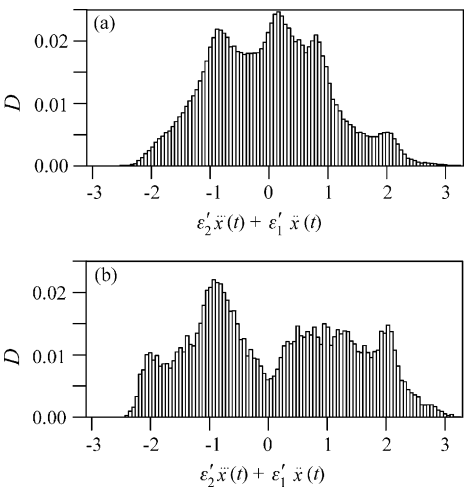

Fig. 8. Distribution D of the sum $\varepsilon_2'\dddot{x}(t) + \varepsilon_1'\ddot{x}(t)$ for all points of the experimental time series (a) and for the extremal points (b).

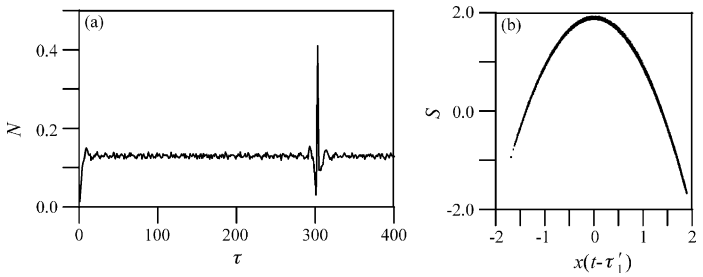

Fig. 9. (a) Number N of pairs of extrema in the time series of Eq. (15) separated in time by τ, as a function of τ. $N(\tau)$ is normalized to the total number of extrema in the time series. $N_{\min}(\tau) = N(301)$. (b) The recovered nonlinear function. $S = \varepsilon_3'\dddot{x}(t) + \varepsilon_2'\ddot{x}(t) + \varepsilon_1'\dot{x}(t) + x(t)$.

The next example is the method application to time series of the third-order time-delay system

$$\varepsilon_3\dddot{x}(t) + \varepsilon_2\ddot{x}(t) + \varepsilon_1\dot{x}(t) = -x(t) + f(x(t-\tau_1)) \tag{15}$$

with quadratic nonlinear function $f(x) = \lambda - x^2$, where λ is the parameter of nonlinearity. The parameters of the system (15) are chosen to be $\tau_1 = 300$, $\lambda = 1.9$, $\varepsilon_1 = 4$, $\varepsilon_2 = 5$ and $\varepsilon_3 = 2$. The $N(\tau)$ plot, constructed with the step of τ variation equal to unity, shows the absolute minimum at $\tau_1' = 301$ (Fig. 9(a)). The minimum of $N(\tau)$ tends to $\tau_1 = 300$ as the parameters ε_i decrease and shifts to larger τ as ε_i increase. For example, we obtain $\tau_1' = 300$ at $\varepsilon_1 = 2.5$, $\varepsilon_2 = 2$ and $\varepsilon_3 = 0.5$, and $\tau_1' = 302$ at $\varepsilon_1 = 8$, $\varepsilon_2 = 17$ and $\varepsilon_3 = 10$. The higher is the order of the time-delay system (12), the more parameters are to be fitted. This problem is typical in high-dimensional search space [25]. As the result, the time of computation significantly increases. Since our procedure of the parameters estimation involves numerical calculation of the derivatives, the quality of reconstruction deteriorates with the increase of the time-delay system order, resulting in the necessity to calculate more high-order derivatives. In Fig. 9(b) the recovered nonlinear function of Eq. (15) is shown. The quality of this function recovery is worse than the quality of reconstruction for the first-order time-delay systems (8) and (11) (Figs. 3 and 6).

6. Recovery of time-delay systems with two coexisting delays

Let us consider now a time-delay system with two different delay times τ_1 and τ_2

$$\dot{x}(t) = F(x(t), x(t-\tau_1), x(t-\tau_2)). \tag{16}$$

Differentiation of Eq. (16) with respect to t gives

$$\ddot{x}(t) = \frac{\partial F}{\partial x(t)}\dot{x}(t) + \frac{\partial F}{\partial x(t-\tau_1)}\dot{x}(t-\tau_1) + \frac{\partial F}{\partial x(t-\tau_2)}\dot{x}(t-\tau_2). \tag{17}$$

Similarly to temporal realization of Eq. (4), the realization $x(t)$ of Eq. (16) has mainly quadratic extrema and therefore $\dot{x}(t) = 0$ and $\ddot{x}(t) \neq 0$ at the extremal points. Hence, if $\dot{x}(t) = 0$, the condition

$$a\dot{x}(t-\tau_1) + b\dot{x}(t-\tau_2) \neq 0 \tag{18}$$

must be fulfilled, where $a = \partial F(x(t), x(t-\tau_1), x(t-\tau_2))/\partial x(t-\tau_1)$ and $b = \partial F(x(t), x(t-\tau_1), x(t-\tau_2))/\partial x(t-\tau_2)$. The condition (18) can be satisfied only if $\dot{x}(t-\tau_1) \neq 0$ or/and $\dot{x}(t-\tau_2) \neq 0$. By this is meant that the derivatives $\dot{x}(t)$ and $\dot{x}(t-\tau_1)$, or $\dot{x}(t)$ and $\dot{x}(t-\tau_2)$ do not vanish simultaneously. As the result, the number of extrema separated in time by τ_1 and τ_2 from a quadratic extremum must be appreciably less than the number of extrema separated in time by other values of τ and hence, the $N(\tau)$ plot will demonstrate pronounced minima at $\tau = \tau_1$ and $\tau = \tau_2$. Compared to the method of optimal transformations used in Ref. [19] for the recovery of two delays our method requires longer time series, but it is significantly more simple and does not need preprocessing of the data as for example, adaptive partitioning of data used in Ref. [19].

We illustrate the procedure for estimating the other characteristics of time-delay system with two delays from time series for the system governed by the following equation

$$\varepsilon_1\dot{x}(t) = -x(t) + f_1(x(t-\tau_1)) + f_2(x(t-\tau_2)). \tag{19}$$

Differentiation of Eq. (19) with respect to t gives

$$\varepsilon_1\ddot{x}(t) = -\dot{x}(t) + \frac{\partial f_1(x(t-\tau_1))}{\partial x(t-\tau_1)}\dot{x}(t-\tau_1) + \frac{\partial f_2(x(t-\tau_2))}{\partial x(t-\tau_2)}\dot{x}(t-\tau_2). \quad (20)$$

From Eq. (20) it follows that if

$$\dot{x}(t-\tau_1) = \dot{x}(t-\tau_2) = 0 \quad (21)$$

then $\varepsilon_1\ddot{x}(t) = -\dot{x}(t)$ and

$$\varepsilon_1 = -\frac{\dot{x}(t)}{\ddot{x}(t)}. \quad (22)$$

Thus, to estimate the parameter ε_1 one can find the points of $x(t)$ satisfying condition (21), define for them the first and the second derivatives, calculate ε_1 using Eq. (22), and conduct averaging. Note that one can also use Eq. (22) for the recovery of ε_1 in the case of a single delay, but such estimation uses only the points with $\dot{x}(t-\tau_1) = 0$ and is not so accurate as the method considered in Section 3. To reduce the computation time we use Eq. (22) for the first approximation of the parameter ε_1 and improve this estimation later on.

To recover the nonlinear functions f_1 and f_2 we project the trajectory generated by Eq. (19) to a three-dimensional space $(x(t-\tau_1), x(t-\tau_2), \varepsilon_1\dot{x}(t)+x(t))$. In this space the projected trajectory is confined to a two-dimensional surface since according to Eq. (19)

$$\varepsilon_1\dot{x}(t) + x(t) = f_1(x(t-\tau_1)) + f_2(x(t-\tau_2)). \quad (23)$$

The section of this surface with the $x(t-\tau_2) = \text{const}$ plane enables one to recover the nonlinear function f_1 up to a constant since the points of the section are correlated via $\varepsilon_1\dot{x}(t) + x(t) = f_1(x(t-\tau_1)) + c_1$, where $c_1 = f_2(x(t-\tau_2))$ for some fixed value of $x(t-\tau_2)$. In a similar way one can recover up to a constant the nonlinear function f_2 by intersecting the trajectory projected to the above-mentioned three-dimensional space with the $(t-\tau_1) = \text{const}$ plane. The points of this section are correlated via $\varepsilon_1\dot{x}(t) + x(t) = f_2(x(t-\tau_2)) + c_2$, where $c_2 = f_1(x(t-\tau_1))$ for fixed $x(t-\tau_1)$.

We demonstrate the method efficiency with a generalized Mackey–Glass equation obtained by introducing a further delay,

$$\dot{x}(t) = -bx(t) + \frac{1}{2}\frac{a_1x(t-\tau_1)}{1+x^c(t-\tau_1)} + \frac{1}{2}\frac{a_2x(t-\tau_2)}{1+x^c(t-\tau_2)}. \quad (24)$$

Division of Eq. (24) by b reduces it to Eq. (19) with $\varepsilon_1 = 1/b$. Fig. 10(a) shows the $N(\tau)$ plot for $a_1 = 0.2$, $a_2 = 0.3$, $b = 0.1$, $c = 10$, $\tau_1 = 70$ and $\tau_2 = 300$. The first two most pronounced minima of $N(\tau)$ are observed at $\tau_1' = 69$ and $\tau_2' = 300$. Another distinctive minimum of $N(\tau)$ is observed close to $\tau = \tau_1 + \tau_2$. Processing the points satisfying condition (21) with the recovered values τ_1' and τ_2' we obtain the averaged estimation $\varepsilon_1' = 9.4$ for the parameter $\varepsilon_1 = 1/b = 10$. To reduce inaccuracy in ε_1 determination by formula (22) we exclude from consideration the points with very small values of $\ddot{x}(t)$.

Projecting the time series of Eq. (24) to the three-dimensional space $(x(t-\tau_1'), x(t-\tau_2'), \varepsilon_1'\dot{x}(t)+x(t))$ and constructing the sections of this space with the planes $x(t-\tau_2') = \text{const}$ and $x(t-\tau_1') = \text{const}$ we obtain at these sections the recovered nonlinear functions f_1 and f_2 (Fig. 10(b) and (c)). However, as the result of inaccuracy in estimation of τ_1 and ε_1 the quality of the nonlinear function recovery is not good enough.

To achieve more high quality of the model equation reconstruction we propose the following procedure for the correction of the parameters. Varying τ_1 in a small vicinity of $\tau_1' = 69$ we project the time series to several three-dimensional $(x(t-\tau_1), x(t-\tau_2'), \varepsilon_1'\dot{x}(t)+x(t))$ spaces and plot their sections with the $x(t-\tau_2') = \text{const}$ plane, searching for a section, which points contract to a curve demonstrating almost single-valued dependence. As a quantitative criterion of single-valuedness we use the minimal length of a line $L(\tau_1)$ connecting all points of the section ordered with respect to abscissa. The $L(\tau_1)$ plot demonstrates the minimum at $\hat{\tau}_1 = 70$ (Fig. 11(a)). Similarly, the correction of the delay time τ_2 is performed. We project the time series to $(x(t-\hat{\tau}_1), x(t-\tau_2), \varepsilon_1'\dot{x}(t)+x(t))$ spaces under variation of τ_2 in the vicinity of $\tau_2' = 300$ and plot the sections $x(t-\hat{\tau}_1) = \text{const}$. Note, that for these sections the corrected delay time $\hat{\tau}_1 = 70$ is used. The minimum of $L(\tau_2)$ takes place at $\hat{\tau}_2 = 300$ (Fig. 11(b)). In the general case if $\hat{\tau}_2 \neq \tau_2'$, the procedure of τ_1 revision is repeated by plotting the sections of

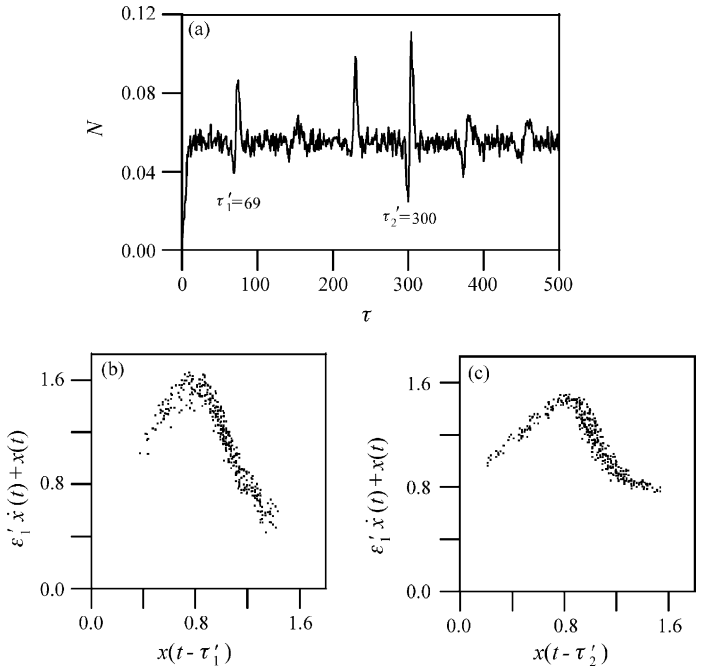

Fig. 10. (a) Number N of pairs of extrema in the time series of Eq. (24) separated in time by τ, as a function of τ. $N(\tau)$ is normalized to the total number of extrema in the time series. (b) The recovered nonlinear function f_1. (c) The recovered nonlinear function f_2.

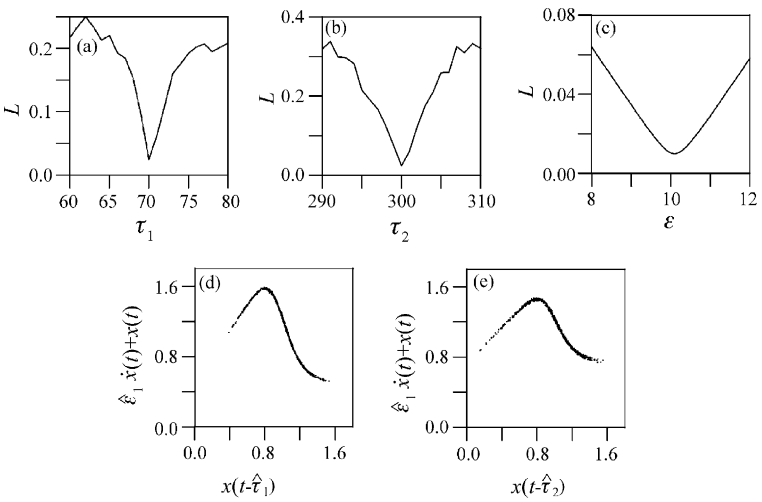

Fig. 11. (a) Length L of a line connecting points ordered with respect to abscissa in the $x(t-\tau_2')=1$ section, as a function of τ_1. $L_{\min}(\tau_1)=L(70)$. (b) Length L of a line connecting points ordered with respect to abscissa in the $x(t-\hat{\tau}_1)=1$ section, as a function of τ_2. $L_{\min}(\tau_2)=L(300)$. (c) Length L of a line connecting points ordered with respect to abscissa in the $x(t-\hat{\tau}_2)=1$ section, as a function of ε. $L_{\min}(\varepsilon)=L(10.1)$. (d) Nonlinear function f_1 recovered up to the constant $\hat{c}_1=f_2(x(t-\hat{\tau}_2))$, where $x(t-\hat{\tau}_2)=1$. (e) Nonlinear function f_2 recovered up to the constant $\hat{c}_2=f_1(x(t-\hat{\tau}_1))$, where $x(t-\hat{\tau}_1)=1$.

the embedding spaces with the $x(t-\hat{\tau}_2) = \text{const}$ plane with the corrected delay time $\hat{\tau}_2$. Successive correction of τ_1 and τ_2 is continued until the parameters cease changing. For small deviations of initial estimates τ_1' and τ_2' from the true delay times the procedure is converging and allows one to define both delay times accurately.

After revision of the delay times the parameter ε_1 should be corrected. Its new estimate $\hat{\varepsilon}_1$ can be obtained by formula (22). However, a more reliable estimation is the one using all points of one of the section. To obtain it we project the time series to $(x(t-\hat{\tau}_1), x(t-\hat{\tau}_2), \varepsilon\dot{x}(t)+x(t))$ spaces under variation of ε in the vicinity of ε_1', searching for a single-valued dependence in the section $x(t-\hat{\tau}_1) = \text{const}$ or in the section $x(t-\hat{\tau}_2) = \text{const}$. The $L(\varepsilon)$ plot shows the minimum at $\hat{\varepsilon}_1 = 10.1$ (Fig. 11(c)). In Fig. 11 the values of $L(\varepsilon)$, $L(\tau_1)$ and $L(\tau_2)$ are normalized to the number of points in the corresponding section. Note, that the proposed procedure of the successive correction of the parameters needs in several orders of magnitude smaller time of computation than the method of simultaneous selection of the parameters ε_1, τ_1 and τ_2 for the three-dimensional embedding space $(x(t-\tau_1), x(t-\tau_2), \varepsilon_1\dot{x}(t)+x(t))$.

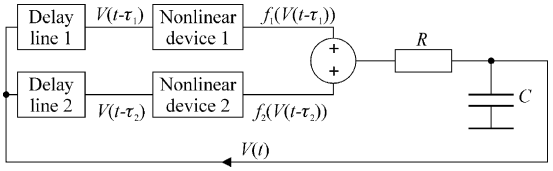

Fig. 12. Block diagram of the electronic oscillator with two delays.

Fig. 11(d) and (e) illustrate the reconstructed nonlinear functions of the system with two coexisting delays (24) for the corrected parameters $\hat{\varepsilon}_1 = 10.1$, $\hat{\tau}_1 = 70$ and $\hat{\tau}_2 = 300$. The nonlinear functions f_1 and f_2 are recovered up to the constant by plotting the sections of the two-dimensional surface described by Eq. (23). To investigate the method efficiency in the presence of noise we apply it to noisy data and found that the method provides sufficiently accurate reconstruction of the investigated system for noise levels up to 10% (the signal-to-noise ratio is 20 dB).

As another example, we consider the method application to experimental time series produced by a setup with two delays. A block diagram of the electronic scheme is shown in Fig. 12. This electronic oscillator is governed by Eq. (23), where $x(t)$ is the voltage at the input of the delay lines, $x(t-\tau_1)$ and $x(t-\tau_2)$

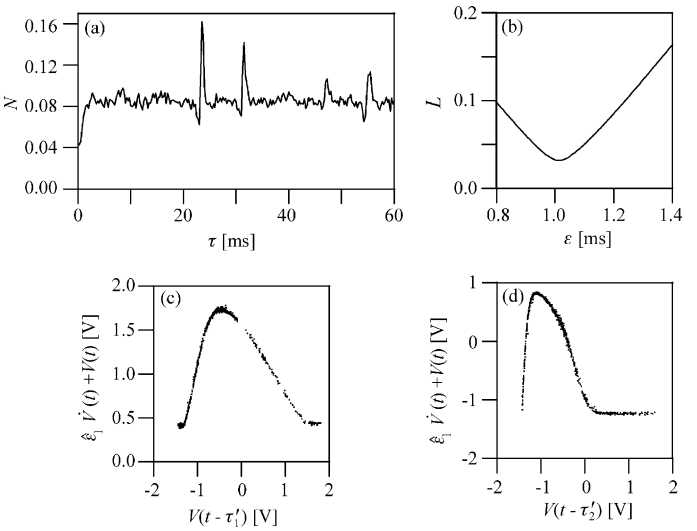

Fig. 13. (a) Number N of pairs of extrema in the time series of the experimental system with two delays separated in time by τ. $N(\tau)$ is normalized to the total number of extrema in the time series. (b) Length L of a line connecting points ordered with respect to abscissa in the $V(t-\tau_1') = -1.1$ V section, as a function of ε. $L(\varepsilon)$ is normalized to the number of points in the section. $L_{\min}(\varepsilon) = L(1.01\,\text{ms})$. (c) Nonlinear function f_1 recovered up to the constant $c_1 = f_2(V(t-\tau_2'))$, where $V(t-\tau_2') = -0.8$ V. (d) Nonlinear function f_2 recovered up to the constant $c_2 = f_1(V(t-\tau_1'))$, where $V(t-\tau_1') = -1.1$ V.

are the output voltages of the first and the second delay lines, respectively, and $\varepsilon_1 = RC$. The time series of $V(t)$ are recorded at $\tau_1 = 23.0$ ms, $\tau_2 = 31.1$ ms and $\varepsilon_1 = 1.007$ ms with the sampling frequency $f_s = 4$ kHz. The $N(\tau)$ plot, constructed with the step of τ variation equal to the sampling time $T_s = 0.25$ ms, demonstrates the first two most pronounced minima at $\tau_1' = 23.0$ ms and $\tau_2' = 31.0$ ms (Fig. 13(a)). These values of the delay times allow us to obtain the estimation $\varepsilon_1' = 1.16$ ms from Eqs. (21) and (22). To obtain the estimation of ε_1 using more number of points we project the time series to $(V(t-\tau_1'), V(t-\tau_2'), \varepsilon\dot{V}(t) + V(t))$ spaces under variation of ε in the vicinity of ε_1', searching for a single-valued dependence in the section $V(t-\tau_1') = \text{const}$. The $L(\varepsilon)$ plot, constructed with the step of ε variation equal to 0.01 ms, demonstrates the minimum at $\hat{\varepsilon}_1 = 1.01$ ms (Fig. 13(b)). The recovered nonlinear functions f_1 and f_2 are presented in Fig. 13(c) and (d), respectively, for $\tau_1' = 23.0$ ms, $\tau_2' = 31.0$ ms and $\hat{\varepsilon}_1 = 1.01$ ms. These functions are recovered up to a constant and are sufficiently close to the true transfer functions of the nonlinear elements of the scheme.

7. Conclusion

We have proposed the methods for reconstructing various classes of time-delay systems from chaotic time series. These methods are based on the statistical analysis of time intervals between extrema in the time series and the projection of infinite-dimensional phase space of the time-delay system to suitably chosen low-dimensional subspaces. The methods can be applied to the systems of different nature if these systems have similar structure of model equations. The proposed techniques allow one to estimate the delay times, the parameters characterizing the inertial properties of the system and the nonlinear functions even in the presence of sufficiently high noise. The method of the delay time definition uses only operations of comparing and adding. It needs neither ordering of data, nor calculation of approximation error or certain measure of complexity of the trajectory and therefore it does not need significant time of computation. For the systems with a single delay time the procedures proposed for the nonlinear function recovery and estimation of the parameters characterizing the inertial properties of the system use all points of the time series. It allows one to successively apply the method to short time series even in the regimes of weakly developed chaos.

It is shown that the model equations of the ring time-delay systems can be reconstructed from time series of various dynamical variables measured at different points of the time-delay system. The methods efficiency is illustrated by the reconstruction of time-delay differential equations from their time series including the case of noise presence and by modelling real time-delayed feedback systems from experimental data.

Acknowledgements

This work is supported by the Russian Foundation for Basic Research, Grant No. 03-02-17593. BPB and ASK acknowledge support from U.S. Civilian Research Development Foundation for the Independent States of the Former Soviet Union, Award No. REC-006, and MDP acknowledges support from INTAS, Grant No. 03-55-920.

References

[1] J.K. Hale, S.M.V. Lunel, Introduction to Functional Differential Equations, Springer, New York, 1993.
[2] Y. Kuang, Delay Differential Equations With Applications in Population Dynamics, Academic Press, Boston, 1993.
[3] K. Ikeda, K. Matsumoto, High-dimensional chaotic behavior in systems with time-delayed feedback, Physica D 29 (1987) 223–235.
[4] K. Ikeda, Multiple-valued stationary state and its instability of the transmitted light by a ring cavity system, Opt. Commun. 30 (1979) 257–261.
[5] R. Lang, K. Kobayashi, External optical feedback effects on semiconductor injection lasers, IEEE J. Quantum Electron. 16 (1980) 347–355.
[6] M.C. Mackey, L. Glass, Oscillations and chaos in physiological control systems, Science 197 (1977) 287–289.
[7] G.A. Bocharov, F.A. Rihan, Numerical modelling in biosciences using delay differential equations, J. Comp. Appl. Math. 125 (2000) 183–199.
[8] J.D. Farmer, Chaotic attractors of an infinite-dimensional dynamical system, Physica D 4 (1982) 366–393.
[9] A.C. Fowler, G. Kember, Delay recognition in chaotic time series, Phys. Lett. A 175 (1993) 402–408.
[10] R. Hegger, M.J. Bünner, H. Kantz, A. Giaquinta, Identifying and modeling delay feedback systems, Phys. Rev. Lett. 81 (1998) 558–561.
[11] C. Zhou, C.-H. Lai, Extracting messages masked by chaotic signals of time-delay systems, Phys. Rev. E 60 (1999) 320–323.

[12] V.S. Udaltsov, J.-P. Goedgebuer, L. Larger, J.-B. Cuenot, P. Levy, W.T. Rhodes, Cracking chaos-based encryption systems ruled by nonlinear time delay differential equations, Phys. Lett. A 308 (2003) 54–60.
[13] Y.-C. Tian, F. Gao, Extraction of delay information from chaotic time series based on information entropy, Physica D 108 (1997) 113–118.
[14] D.T. Kaplan, L. Glass, Coarse-grained embeddings of time series: random walks, Gaussian random process, and deterministic chaos, Physica D 64 (1993) 431–454.
[15] M.J. Bünner, M. Popp, Th. Meyer, A. Kittel, U. Rau, J. Parisi, Recovery of scalar time-delay systems from time series, Phys. Lett. A 211 (1996) 345–349.
[16] M.J. Bünner, M. Popp, Th. Meyer, A. Kittel, J. Parisi, Tool to recover scalar time-delay systems from experimental time series, Phys. Rev. E 54 (1996) 3082–3085.
[17] M.J. Bünner, Th. Meyer, A. Kittel, J. Parisi, Recovery of the time-evolution equation of time-delay systems from time series, Phys. Rev. E 56 (1997) 5083–5089.
[18] M.J. Bünner, M. Ciofini, A. Giaquinta, R. Hegger, H. Kantz, R. Meucci, A. Politi, Reconstruction of systems with delayed feedback: (I) Theory, Eur. Phys. J. D 10 (2000) 165–176.
[19] H. Voss, J. Kurths, Reconstruction of non-linear time delay models from data by the use of optimal transformations, Phys. Lett. A 234 (1997) 336–344.
[20] S.P. Ellner, B.E. Kendall, S.N. Wood, E. McCauley, C.J. Briggs, Inferring mechanism from time-series data: delay differential equations, Physica D 110 (1997) 182–194.
[21] H. Voss, J. Kurths, Reconstruction of nonlinear time-delayed feedback models from optical data, Chaos Solitons Fractals 10 (1999) 805–809.
[22] B.P. Bezruchko, A.S. Karavaev, V.I. Ponomarenko, M.D. Prokhorov, Reconstruction of time-delay systems from chaotic time series, Phys. Rev. E 64 (2001) 056216.
[23] V.I. Ponomarenko, M.D. Prokhorov, Extracting information masked by the chaotic signal of a time-delay system, Phys. Rev. E 66 (2002) 026215.
[24] B. Mensour, A. Longtin, Synchronization of delay-differential equations with application to private communication, Phys. Lett. A 244 (1998) 59–70.
[25] P.J. Green, B.W. Silverman, Nonparametric Regression and Generalized Linear Models, Chapman and Hall, London, 1994.